Weak Integrability Breaking: Chaos with Integrability Signature in Coherent Diffusion

Marko Žnidarič
Physics Department, Faculty of Mathematics and Physics, University of Ljubljana, 1000 Ljubljana, Slovenia

(Received 23 June 2020; accepted 5 October 2020; published 28 October 2020)

We study how perturbations affect dynamics of integrable many-body quantum systems, causing transition from integrability to chaos. Looking at spin transport in the Heisenberg chain with impurities we find that in the thermodynamic limit transport gets diffusive already at an infinitesimal perturbation. Small extensive perturbations therefore cause an immediate transition from integrability to chaos. Nevertheless, there is a remnant of integrability encoded in the dependence of the diffusion constant on the impurity density, namely, at small densities it is proportional to the square root of the inverse density, instead of to the inverse density as would follow from Matthiessen's rule. We show that Matthiessen's rule has to be modified in nonballistic systems. Results also highlight a nontrivial role of interacting scattering on a single impurity, and that there is a regime where adding more impurities can actually increase transport.

DOI: 10.1103/PhysRevLett.125.180605

Integrable systems form one of the cornerstones on which our understanding of nature rests. Their solvability leads to an enhanced understanding of that particular system, while on the other hand often enough such simplified models do actually describe realistic systems with a sufficient precision. An example is physics at low energies where description in terms of non- or weakly interacting quasiparticles often applies, and if on top of that the "environmental" effects are small, one has a perfect experimental test bed of integrable physics. The last decade has seen a broad expansion of interest to genuine many-body systems with interactions that are not integrable and to generic high energy states. A pertinent question is, how, if at all, is integrability that is often only weakly broken, reflected in properties of a nonintegrable model as probed in an out-of-equilibrium situation [1,2]?

We study two questions: (i) breaking of integrability in a many-body system and, in particular, at what perturbation strength does one get a full generic complexity associated with ergodicity, decay of correlations and in our case diffusive transport, and (ii) after integrability is broken and transport goes from nondiffusive (typical of integrable systems [3]) to diffusive, is there some remaining signature of the parent integrability, or it vanishes completely, making integrable systems an utterly singular notion that immediately goes into "featureless" diffusion in the thermodynamic limit (TDL)? We find that the critical perturbation strength for the transition from integrability to chaos is zero in the TDL. Nevertheless, the original integrability is still reflected in a modified Matthiessen's rule—in general the diffusion constant is not simply inversely proportional to the density of impurities.

From a single-particle quantum chaos [4], or few-degrees-of-freedom classical systems, we know that the transition from integrability to chaos typically happens at a finite perturbation strength (for classical systems the KAM theorem makes that rigorous [5]). For many-body quantum systems one might expect that the transition strength will instead go to zero in the TDL, results though are not always as clear cut despite a long history, e.g., Refs. [6–9]. For instance, while traditional criteria of single-particle quantum chaos like the nearest-neighbor level spacing distribution (LSD) typically do show a transition at zero perturbation strength [7,8,10] in the TDL, looking at the decay of correlation functions there are observations of nonergodicity at finite perturbations [9]. An important point to keep in mind is that the LSD probes unobservable exponentially small energy scales and is not always a suitable indicator of complexity (chaos). For instance, a small local perturbation suffices to make a system "chaotic" according to the LSD [11–14], despite transport remaining that of an integrable model (ballistic) [12]. Coexistence of chaotic LSD and nonergodic wave functions can be observed also in disordered systems [15,16]. It is therefore important to better understand integrability to chaos transition in many-body systems in terms of observables in as large systems as possible in order to correctly account for long timescales and length scales emerging at weak perturbations, a problem which can plague exact diagonalization studies of the transition.

We do that by studying transport in the Heisenberg spin-1/2 chain with integrability-breaking impurities (Fig. 1). The model is appealing for a number of reasons. (i) Without impurities it is integrable, with spin transport at high temperature well understood. (ii) The chosen perturbation allows us to study three different kinds of integrability breaking: the interaction Δ, the impurity strength h, and the impurity density $1/\lambda$. (iii) The model is experimentally relevant, realized in a number of spin-chain materials like strontium cuprate, where high heat conductivity measured

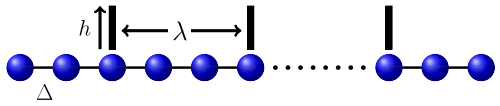

FIG. 1. *XXZ* chain (1) with magnetic field of amplitude h at sites separated by distance λ (shown is $\lambda = 3$).

at low T is attributed to ballistic spin transport along Heisenberg chains [17]. Because crystals are never perfect [18], or by deliberately introducing impurities [19,20], one in fact always deals with the Heisenberg model with low density of impurities—precisely what we study. Transport in the Heisenberg model has also been studied in cold-atoms experiments [21–23] and with neutron scattering [24], promising an even greater controllability in the future. (iv) Importantly, transport at an infinite T can be studied in large systems, avoiding finite-size effects.

What we find is that the faster-than-diffusive spin transport of the integrable model goes upon integrability breaking immediately to diffusion, with a diverging diffusion constant D at small perturbations (see Fig. 2). For dilute impurities, $\lambda \gg 1$, one would expect $D \propto \lambda$ because the scattering on different impurities is independent, making the rates $1/\tau_i$ additive, leading under a simple kinetic Drude formula $D \sim v^2\tau$ to $D \propto \lambda$—the famous Matthiessen's rule [25] that is indeed observed in the mentioned Heisenberg spin-chain materials [20] or, e.g., dilute alloys [25]. What we find, however, is that Matthiessen's rule has to be modified to $D \propto \lambda^{2-z}$, where z is the dynamical transport exponent of the integrable model ($z = \frac{3}{2}$ for the superdiffusive isotropic Heisenberg chain at $T = \infty$). We also find other intriguing features: for $\Delta < 1$ and large λ the diffusion constant has a nontrivial dependence on h that can be explained by interacting scattering on a single impurity, and there is a regime of high impurity density where spin transport gets faster upon increasing the number of impurities.

Because we focus on transport that is defined in the TDL $\lim_{t\to\infty}\lim_{L\to\infty}$ we do not directly probe finite-time behavior. However, one can note that the way D diverges for small perturbations is indicative of relaxation timescales. We therefore expect that the physics we find in D should be also reflected in finite-time phenomena like prethermalization [26]. Another approach dealing with near-integrable systems is using generalized hydrodynamics [27,28] and/or conserved quantities to study dynamics upon weak integrabilty breaking [29–34].

Results.—The anisotropic Heisenberg spin-1/2 chain [35] with periodic impurities is

$$H = \sum_{r=0}^{L-1} \sigma_r^x\sigma_{r+1}^x + \sigma_r^y\sigma_{r+1}^y + \Delta\sigma_r^z\sigma_{r+1}^z + h\sum_{k=1}^{M=L/\lambda} \sigma^z_{[k\frac{L}{M+1}]}, \tag{1}$$

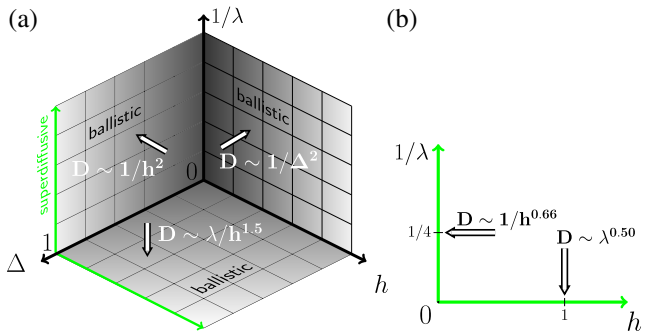

FIG. 2. Summary: (a) When any small parameter h, Δ or $1/\lambda$ is 0 one has known ballistic transport. For nonzero perturbations one gets diffusion with white arrows indicating how diffusion constant D diverges. (b) $\Delta = 1$, where one has superdiffusion (green) without perturbation.

where $M = (L/\lambda)$ is the number of impurities, λ the distance between them, and h the size of magnetic field (see Fig. 1) [36]. We shall focus on spin transport at an infinite temperature and zero magnetization (half-filling). Chaos is a property of generic states and so the ensemble with $T = \infty$ is the most unbiased, and at the same time the easiest to simulate with our numerical method. Without impurities the model is integrable, with spin transport at half-filling and $T = \infty$ being ballistic for $\Delta < 1$ [37–39], and superdiffusive at $\Delta = 1$ [40–42]. Because we will focus on the breaking of this faster-than-diffusive integrable transport to diffusion we shall not consider $\Delta > 1$ where it is diffusive already without impurities [41]. Any nonzero number of impurities makes the model in general nonintegrable [11]. We note that with a single impurity (finite L and $\lambda = \infty$) the spin transport is the same [12] as for the clean integrable model. Previous studies of transport in the Heisenberg model at high-T under various (weak) perturbations include Refs. [43–52].

To numerically assess spin transport we are going to couple the spin chain at first and last sites to magnetization reservoirs described by Lindblad operators $L_1 = \sqrt{\Gamma(1+\mu)}\sigma_0^+$, $L_2 = \sqrt{\Gamma(1-\mu)}\sigma_0^-$, $L_3 = \sqrt{\Gamma(1-\mu)}\sigma_{L-1}^+$, and $L_4 = \sqrt{\Gamma(1+\mu)}\sigma_{L-1}^-$, such that the evolution of the density matrix is described by the Lindblad master equation [53,54]. Its solution converges at long times to a unique nonequilibrium steady state (NESS) whose properties determine transport, in particular the NESS spin current $j = \mathrm{tr}(\rho(2\sigma_k^x\sigma_{k+1}^y - 2\sigma_k^y\sigma_{k+1}^x))$, and magnetization at site k, $z_k = \mathrm{tr}(\rho\sigma_k^z)$. For zero H the chosen Lindblad operators would induce a steady-state $\rho \sim \mathbb{1} + \mu\sigma_0^z$ on the 1st site, and $\rho \sim \mathbb{1} - \mu\sigma_{L-1}^z$ on the last site (independent of Γ). They therefore try to induce magnetization $+\mu$ and $-\mu$, respectively, and so 2μ can be thought of as the driving potential difference. Nonzero H makes dynamics and the NESS nontrivial, with the transport type being encoded in the dependence of j on L, as well as in the shape of the magnetization profile. For diffusive systems in the linear response regime (small μ; we use

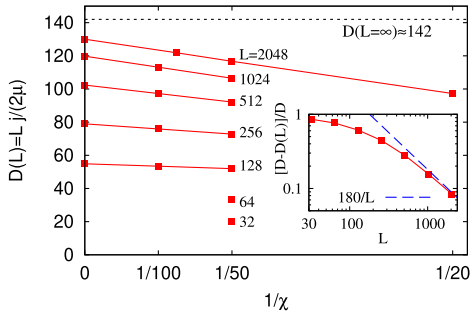

FIG. 3. Determining diffusion constant ($\lambda = 32$, $\Delta = 0.6$, $h = 0.5$). Main plot: convergence with the bond dimension χ of a finite-size value of $D(L)$, together with the extrapolated values plotted at $1/\chi = 0$ (for $L = 32$, 64 no extrapolation is used). Inset: relative precision of $D(L)$ improves as $\sim 1/L$, as predicted [56], but with a large prefactor ≈ 180.

$\mu = 0.1$) the profile will be on average linear [see Fig. 4(c) for an example] while the current will scale as $j \asymp -D(2\mu/L)$, from which one can extract the diffusion constant D. At $\mu = 0$ the NESS is a trivial $\sim \mathbb{1}$ corresponding to an equilibrium $T = \infty$ driving. At $\mu \ll 1$ the NESS is still close to $\mathbb{1}$, energy density is zero, and so the driving probes transport at $T = \infty$ and at zero average magnetization. The coupling strength Γ, which only influences the boundary resistance, is set to $\Gamma = 1$ (see Ref. [55] for more details on μ and Γ). Note that the particular choice of driving does not influence the bulk transport properties, specifically, the extracted diffusion constant is the same as the one obtained from the Green-Kubo approach [56].

To represent a solution of the Lindblad equation $\rho(t)$ efficiently we use a matrix product operator ansatz with matrices of size χ and the tDMRG method [57] to evolve $\rho(t)$ in time. The method has proved itself in the past, see, e.g., Ref. [58] and references therein for more details, and allows at "easy" parameter values to simulate systems as large as $L \approx 2000$ sites. The crucial parameter that determines its efficiency is χ. The largest χ we can afford is about $\chi \sim 100$ at $L \sim 1000$ ($\chi \approx 300$ for some smaller L). For parameters where truncation errors are larger we run simulations at different χ and use extrapolation to gain in accuracy (Fig. 3).

We first check the isotropic chain, $\Delta = 1$. Fixing $\lambda = 4$ we calculate the NESS for increasingly smaller values of magnetic field h, each time studying the scaling of j with L. In all cases we find diffusive $j \sim 1/L$, see Ref. [55] for data. In Fig. 4(a) we plot the obtained $D(h)$. According to Fermi's golden rule, the scattering rate should scale as $1/\tau \sim h^2$. In a system with dynamical exponent z, defined by the scaling of distance with time as $x^z \sim t$ (and the NESS current as $j \sim 1/L^{z-1}$), e.g., $z = 1$ for ballistic, $z = 2$ for diffusion, the scattering length should go as $l \sim 1/h^{2/z}$. For the isotropic model at an infinite temperature $z = \frac{3}{2}$ [40], predicting divergence $D \sim 1/h^{2/3}$, similarly as for a disordered potential [58]. Numerical results in Fig. 4(a) agree with that scaling (the agreement is achieved only at very small $h \lesssim 0.3$; at larger h the scaling power is larger). From an experimental point of view we would in particular like to understand the case of dilute impurities, $\lambda \gg 1$. To that end we plot in Fig. 4(b) the scaling of D with λ for several values of h. We see that D is not proportional to λ. This is due to nonballistic transport between impurities and can be explained as follows. Focusing on a segment of length λ between two impurities, the magnetization difference across the segment is $\delta z \approx 2\mu/M = 2\mu\lambda/L$ and will drive the current of size $j \sim \delta z/\lambda^{z-1}$ through the segment. The last relation comes because an excitation needs time $\sim\lambda^z$ to travel across the length λ, resulting in a current $\sim\lambda/\lambda^z$ (at fixed excitation density there are $\sim\lambda$ excitations in a segment of length λ). The NESS current therefore scales as $j \sim (2\mu/L)(\lambda/\lambda^{z-1})$, giving

$$D \sim \lambda^{2-z}. \tag{2}$$

Using $z = \frac{3}{2}$ of the isotropic model we see that the resulting $D \sim \sqrt{\lambda}$ agrees within numerical errors with data in Fig. 4(b). Deviations seen for smaller $h = 0.6$, 0.3 are presumably due to the scattering length being larger than $\lambda = 32$, which is the largest λ we can reliably simulate. In Fig. 4(c) we plot the magnetization profile across a chain, showing nonequilibrium spikes at locations of impurities (spikes are not visible for all parameters, and are typically stronger at smaller D).

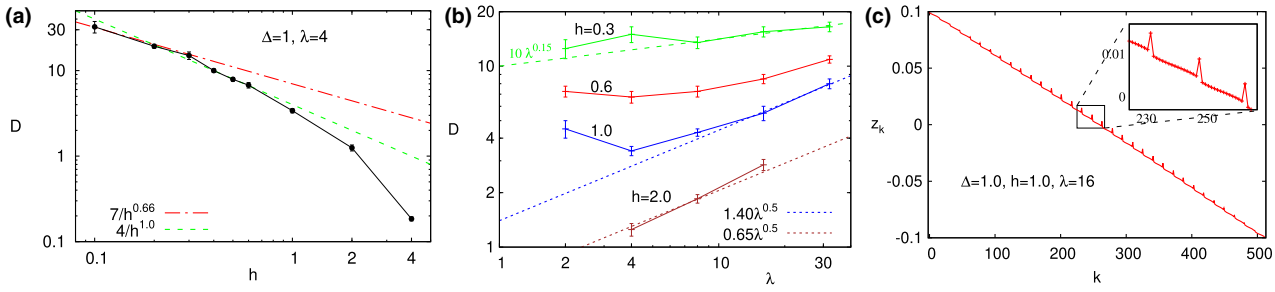

FIG. 4. Isotropic chain, $\Delta = 1$. (a) Dependence of D on h for $\lambda = 4$. (b) Diffusion constant scaling with λ; for $\lambda \gg 1$ it is not proportional to λ (inverse impurity density) but is rather $D \sim \lambda^{0.5}$. (c) Magnetization profile has spikes at impurities ($h = 1$, $\lambda = 16$, $L = 512$).

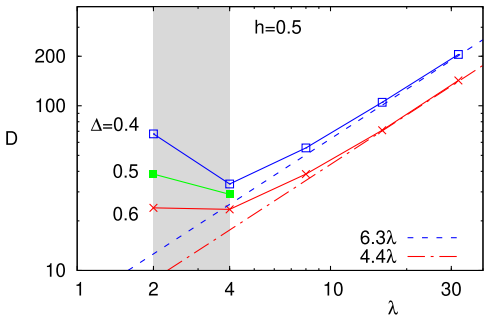

FIG. 5. Diffusion scaling for $\Delta < 1$ ($h = 0.5$). For $\lambda \gg 1$ it is linear, with the prefactor given by a single-impurity physics (Fig. 6), while in the shaded strip D counterintuitively increases by increasing impurities.

Next, we focus on $\Delta < 1$ where the integrable model is ballistic. Fixing $\lambda = 4$, we have two possible small perturbations, either taking small Δ, or small h. We again find that small integrability breaking immediately leads to diffusion. For the two perturbation types, Fermi's golden rule gives the scattering length $l \sim 1/\Delta^2$, or $l \sim 1/h^2$, leading to diffusion constant divergence $D \sim 1/\Delta^2$, or $D \sim 1/h^2$, respectively. This is inline with numerical data; see Ref. [55] for data. Increasing λ at fixed h, and using ballistic $z = 1$, Eq. (2) predicts $D \propto \lambda$ at $\lambda \gg 1$, which agrees with numerics (Fig. 5). What is interesting is the behavior at small λ. Between $\lambda = 2$ and 4 the diffusion constant increases by decreasing λ, meaning that the transport gets faster when we add more impurities. The effect is more prominent at small Δ, and was also visible at $h = 1$ in the isotropic case [Fig. 4(b)]. Let us now focus on $\lambda \gg 1$ and in particular on how D depends on parameters. Using the same argument as in deriving Eq. (2) we can see that between rare impurities the magnetization profile will be flat, with a jump happening only at impurities [Fig. 6(a)]. We also observe that at $\lambda \gg 1$ it does not matter whether impurities are equidistant, like in our simulations, or at random positions—D is the same in both cases (the same holds at $\Delta = 1$). Therefore one should be able to get D just from studying the size of the jump at a single impurity. This is what we do in Fig. 6(c). Placing the single impurity at the middle of the chain, we study how the jump size dz scales with h, and, in particular, how a single-impurity resistance $R_{\text{single}} = dz/j$ scales. We determine dz from the 5 central sites around the impurity (for those the profile is independent of L in the TDL). Numerics indicates that $R_{\text{single}} \sim h^{1.5}$ at small h [Fig. 6(b)]. In the noninteracting case $\Delta = 0$ one can solve the corresponding Lindblad equation exactly (following, e.g., Ref. [59]), obtaining the odd-L NESS values $j = 4\mu[\Gamma + 1/\Gamma]/[(\Gamma + 1/\Gamma)^2 + h^2]$, $z_{1,\ldots,(L-1)/2-1} = -z_{(L-1)/2+1,\ldots,L-2} = \mu h^2/[(\Gamma + 1/\Gamma)^2 + h^2]$, $z_0 = -z_{L-1} = \mu[1 + \Gamma^2 + h^2]/[(\Gamma + 1/\Gamma)^2 + h^2]$, $z_{(L-1)/2} = 0$, giving $R_{\text{single}}(\Delta = 0) = h^2/[2(\Gamma + 1/\Gamma)]$ (the scaling of current with h in the single-impurity situation, including at $\Delta = 0$, was numerically studied in Ref. [12]). We see that the power ≈ 1.5 in R_{single} at $\Delta = 0.6$ is different than 2 obtained at $\Delta = 0$. It is also different than the scaling power $D \sim 1/h^{0.66}$ at $\Delta = 1$ (see Supplemental Material [55] for data). It very weakly, if at all, depends on Δ and could therefore be discontinuous at $\Delta = 0$ and $\Delta = 1$ (see Ref. [55]). Scattering on a single impurity in an interacting wire therefore seems to be qualitatively different than in a noninteracting one; we were not able to obtain the power ≈ 1.5 using perturbation theory, leaving this as an interesting problem. R_{single} can now be used to calculate the diffusion constant for $\lambda \gg 1$ in a system that is ballistic without impurities (e.g., $\Delta < 1$), obtaining

$$D = \lambda / R_{\text{single}}. \tag{3}$$

Data in Fig. 6(b) for full many-impurity numerics agree with that well (due to numerical errors the accuracy of the fitted power 1.5 is about 10%). We have an interesting situation where D is very sensitive to having either $\Delta = 0$, or $\Delta = 1$. Changing the interaction Δ just a little away from either of

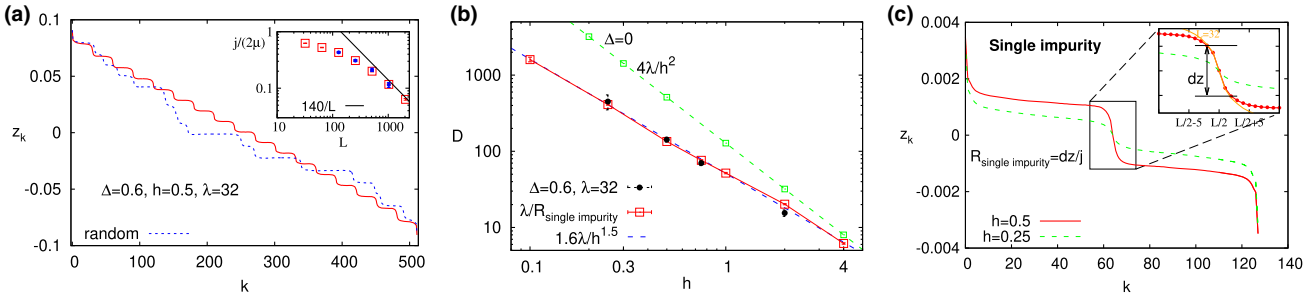

FIG. 6. Anisotropic XXZ with $\Delta = 0.6$. (a) Magnetization profile for $h = 0.5$ and $\lambda = 32$ in a chain with $L = 512$ (red), and for randomly placed $L/\lambda = 16$ impurities (dashed blue). Inset: scaling of the NESS current with L giving $D \approx 140$. Blue points (overlapping with red squares for $\lambda = 32$) show the current for the random case. (b) Scaling of $D(h)$ for $\lambda = 32$ (4 black circles). Red squares are obtained (no fitting parameters) from the single-impurity scattering in frame (c). Green squares is the exact noninteracting result for R_{single}. (c) Magnetization profile for a single impurity at the middle site ($\mu = 0.005$). The main plot shows results for $L = 128$ (enlarged also for $L = 32$ and $h = 0.5$). Magnetization jump at the impurity, $dz := z_{L/2-2} - z_{L/2+2}$, and the NESS j is used to plot red squares in frame (b).

the two points changes D drastically. In fact, in the TDL and $\lambda \to \infty$, or $h \to 0$, the relative change is infinite, coming from different scaling of D with λ (2) as well as different scaling of R_{single} with h. As an example, taking chaotic model with $\lambda = 32$ and $h = 0.5$ we can predict that D increases by about tenfold as one changes the interaction from $\Delta = 1$ to $\Delta = 0.8$.

Conclusion.—Using transport at an infinite temperature as an indicator we studied the transition from integrability to chaos in the Heisenberg spin chain with impurities. By large-scale numerical simulations of systems with up to 2000 spins we find that one gets diffusion already for an infinitesimal perturbation strength, in line with a simple Fermi's golden rule. For the important case of dilute impurities we find that the diffusion constant scales as $D \sim \lambda^{2-z}$, where z is the dynamical exponent of the clean integrable model and λ the distance between impurities. In particular, for the isotropic Heisenberg model Matthiessen's rule has to be changed to $D \propto \sqrt{\lambda}$, instead of the usual textbook $D \propto \lambda$. Such scaling arises due to a combination of an anomalous coherent propagation between impurities interspersed by scattering events on impurities. One can obtain D by analyzing scattering on a single impurity in an interacting model. Also interesting is that increasing the impurity density from $(1/\lambda) = \frac{1}{4}$ to $\frac{1}{2}$ can cause diffusion to become faster. D is for $\lambda \gg 1$ very sensitive to being at the isotropic point. We expect our results to hold also at finite (high) temperatures.

Traditionally, the quantum chaos community has focused on looking for signatures of chaos (generic behavior)—here we instead find signatures of integrability (rare behavior) in the form of a modified Matthiessen's rule in an otherwise chaotic model. While we studied a particular model and type of impurities, arguments are general and should hold for other dilute perturbations, e.g., bond disorder [60], and different interacting models with anomalous transport [61–63], perhaps even for the Fibonacci model [64]. Checking the relation (2) for other conserved quantities, like energy, is also an interesting problem.

I would like to acknowledge support by Grants No. J1-1698 and No. P1-0402 from the Slovenian Research Agency, and ERC OMNES (T. Prosen) for computational resources.

[1] I. Bloch, J. Dalibard, and S. Nascimbene, Quantum simulations with ultracold quantum gases, Nat. Phys. **8**, 267 (2012).
[2] A. Polkovnikov, K. Sengupta, A. Silva, and M. Vengalattore, Colloquium: Nonequilibrium dynamics of closed interacting quantum systems, Rev. Mod. Phys. **83**, 863 (2011).
[3] X. Zotos, F. Naef, and P. Prelovšek, Transport and conservation laws, Phys. Rev. B **55**, 11029 (1997).
[4] F. Haake, *Quantum Signatures of Chaos* (Springer, New York, 2010).
[5] M. C. Gutzwiller, *Chaos in Classical and Quantum Mechanics* (Springer, New York, 1990).
[6] D. Poilblanc, T. Ziman, J. Bellissard, F. Mila, and G. Montambaux, Poisson vs. GOE statistics in integrable and non-integrable quantum hamiltonians, Europhys. Lett. **22**, 537 (1993).
[7] T. C. Hsu and J. C. Angles d'Auriac, Level repulsion in integrable and almost-integrable quantum spin models, Phys. Rev. B **47**, 14291 (1993).
[8] Ph. Jacquod and D. L. Shepelyansky, Emergence of Quantum Chaos in Finite Interacting Fermi Systems, Phys. Rev. Lett. **79**, 1837 (1997).
[9] T. Prosen, Time Evolution of A Quantum Many-Body System: Transition from Integrability to Ergodicity in the Thermodynamic Limit, Phys. Rev. Lett. **80**, 1808 (1998).
[10] L. F. Santos and M. Rigol, Onset of quantum chaos in one-dimensional bosonic and fermionic systems and its relation to thermalization, Phys. Rev. E **81**, 036206 (2010).
[11] L. F. Santos, Integrability of a disordered Heisenberg spin-1/2 chain, J. Phys. A **37**, 4723 (2004).
[12] M. Brenes, E. Mascarenhas, M. Rigol, and J. Goold, High-temperature transport in the XXZ chain in the presence of an impurity, Phys. Rev. B **98**, 235128 (2018).
[13] M. Brenes, T. LeBlond, J. Goold, and M. Rigol, Eigenstate Thermalization in a Locally Perturbed Integrable System, Phys. Rev. Lett. **125**, 070605 (2020).
[14] L. F. Santos, F. Péres-Bernal, and E. J. Torres-Herrera, Speck of chaos, Phys. Rev. Research **2**, 043034 (2020).
[15] T. Micklitz, F. Monteiro, and A. Altland, Nonergodic Extended States in the Sachdev-Ye-Kitaev Model, Phys. Rev. Lett. **123**, 125701 (2019).
[16] A. De Luca, B. L. Altshuler, V. E. Kravtsov, and A. Scardicchio, Anderson Localization on the Bethe Lattice: Nonergodicity of Extended States, Phys. Rev. Lett. **113**, 046806 (2014).
[17] C. Hess, Heat transport of cuprate-based low-dimensional quantum magnets with strong exchange coupling, Phys. Rep. **811**, 1 (2019).
[18] N. Hlubek, X. Zotos, S. Singh, R. Saint-Martin, A. Revcolevschi, B. Büchner, and C. Hess, Spinon heat transport and spin-phonon interaction in the spin-1/2 Heisenberg chain cuprates Sr_2CuO_3 and $SrCuO_2$, J. Stat. Mech. (2012) P03006.
[19] T. Kawamata, N. Takahashi, T. Adachi, T. Noji, K. Kudo, N. Kobayashi, and Y. Koike, Evidence for ballistic thermal conduction in the one-dimensional $S = 1/2$ Heisenberg antiferromagnetic spin system Sr_2CuO_3, J. Phys. Soc. Jpn. **77**, 034607 (2008).
[20] N. Hlubek, R. Saint-Martin, S. Nishimoto, A. Revcolevschi, S.-L. Drechsler, G. Behr, J. Trinckauf, J. E. Hamann-Borrero, J. Geck, B. Büchner, and C. Hess, Bond disorder and breakdown of ballistic heat transport in the spin-1/2 antiferromagnetic Heisenberg chain as seen in Ca-doped $SrCuO_2$, Phys. Rev. B **84**, 214419 (2011).
[21] T. Fukuhara, A. Kantian, M. Endres, M. Cheneau, P. Schauß, S. Hild, D. Bellem, U. Schollwöck, T. Giamarchi, C. Gross, I. Bloch, and S. Kuhr, Quantum dynamics of a mobile spin impurity, Nat. Phys. **9**, 235 (2013).

[22] S. Hild, T. Fukuhara, P. Schauß, J. Zeiher, M. Knap, E. Demler, I. Bloch, and C. Gross, Far-From-Equilibrium Spin Transport in Heisenberg Quantum Magnets, Phys. Rev. Lett. **113**, 147205 (2014).

[23] N. Jepsen, J. Amato-Grill, I. Dimitrova, W. W. Ho, E. Demler, and W. Ketterle, Spin transport in a tunable Heisenberg model realized with ultracold atoms, arXiv:2005.09549.

[24] A. Scheie, N. E. Sherman, M. Dupont, S. E. Nagler, M. B. Stone, G. E. Granroth, J. E. Moore, and D. A. Tennant, Detection of Kardar-Parisi-Zhang hydrodynamics in a quantum Heisenberg spin-1/2 chain, arXiv:2009.13535.

[25] C. Kittel, *Introduction to Solid State Physics* (John Wiley & Sons, New York, 1996).

[26] T. Mori, T. N. Ikeda, E. Kaminishi, and M. Ueda, Thermalization and prethermalization in isolated quantum systems: A theoretical overview, J. Phys. B **51**, 112001 (2018).

[27] B. Bertini, M. Collura, J. De Nardis, and M. Fagotti, Transport in Out-of-Equilibrium XXZ Chains: Exact Profiles of Charges and Currents, Phys. Rev. Lett. **117**, 207201 (2016).

[28] O. A. Castro-Alvaredo, B. Doyon, and T. Yoshimura, Emergent Hydrodynamics in Integrable Quantum Systems out of Equilibrium, Phys. Rev. X **6**, 041065 (2016).

[29] F. Lange, Z. Lenarčič, and A. Rosch, Pumping approximately integrable systems, Nat. Commun. **8**, 15767 (2017).

[30] X. Cao, V. B. Bulchandani, and J. E. Moore, Incomplete Thermalization from Trap-Induced Integrability Breaking: Lessons from Classical Hard Rods, Phys. Rev. Lett. **120**, 164101 (2018).

[31] J.-S. Caux, B. Doyon, J. Dubail, R. Konik, and T. Yoshimura, Hydrodynamics of the interacting Bose gas in the Quantum Newton Cradle setup, SciPost Phys. **6**, 070 (2019).

[32] A. J. Friedman, S. Gopalakrishnan, and R. Vasseur, Diffusive hydrodynaics from integrability breaking, Phys. Rev. B **101**, 180302(R) (2020).

[33] J. Durnin, M. J. Bhaseen, and B. Doyon, Non-equilibrium dynamics and weakly broken integrability, arXiv:2004.11030.

[34] J. Lopez-Piqueres, B. Ware, S. Gopalakrishnan, and R. Vasseur, Hydrodynamics of non-integrable systems from relaxation-time approximation, arXiv:2005.13546.

[35] W. Heisenberg, Zur theorie des ferromagnetismus, Z. Phys. **49**, 619 (1928).

[36] We try to place M equidistant impurities; for finite L the distance between few of them can differ from λ by ± 1, which is, however, irrelevant in the TDL.

[37] X. Zotos, Finite Temperature Drude Weight of the One-Dimensional Spin-1/2 Heisenberg Model, Phys. Rev. Lett. **82**, 1764 (1999).

[38] T. Prosen, Open XXZ Spin Chain: Nonequilibrium Steady State and a Strict Bound on Ballistic Transport, Phys. Rev. Lett. **106**, 217206 (2011).

[39] E. Ilievski and J. De Nardis, Microscopic Origin of Ideal Conductivity in Integrable Quantum Models, Phys. Rev. Lett. **119**, 020602 (2017).

[40] M. Žnidarič, Spin Transport in a One-Dimensional Anisotropic Heisenberg Model, Phys. Rev. Lett. **106**, 220601 (2011).

[41] S. Gopalakrishnan and R. Vasseur, Kinetic Theory of Spin Diffusion and Superdiffusion in XXZ Spin Chains, Phys. Rev. Lett. **122**, 127202 (2019).

[42] V. B. Bulchandani, Kardar-Parisi-Zhang universality from soft gauge modes, Phys. Rev. B **101**, 041411(R) (2020).

[43] X. Zotos and P. Prelovšek, Evidence for ideal insulating or conducting state in a one-dimensional integrable system, Phys. Rev. B **53**, 983 (1996).

[44] J. V. Alvarez and C. Gros, Low-Temperature Transport in Heisenberg Chains, Phys. Rev. Lett. **88**, 077203 (2002).

[45] F. Heidrich-Meisner, A. Honecker, D. C. Cabra, and W. Brenig, Zero-frequency transport properties of one-dimensional spin-1/2 systems, Phys. Rev. B **68**, 134436 (2003).

[46] S. Mukerjee, V. Oganesyan, and D. Huse, Statistical theory of transport by strongly interacting lattice fermions, Phys. Rev. B **73**, 035113 (2006).

[47] P. Jung and A. Rosch, Spin conductivity in almost integrable spin chains, Phys. Rev. B **76**, 245108 (2007).

[48] Y. Huang, C. Karrasch, and J. E. Moore, Scaling of electrical and thermal conductivities in an almost integrable chain, Phys. Rev. B **88**, 115126 (2013).

[49] R. Steinigeweg, J. Gemmer, and W. Brenig, Spin and energy currents in integrable and nonintegrable spin-1/2 chains: A typicality approach to real-time autocorrelations, Phys. Rev.B **91**, 104404 (2015).

[50] R. Steinigeweg, J. Herbrych, X. Zotos, and W. Brenig, Heat Conductivity of the Heisenberg Spin-1/2 Ladder: From Weak to Strong Breaking of Integrability, Phys. Rev. Lett. **116**, 017202 (2016).

[51] J. De Nardis, M. Medenjak, C. Karrasch, and E. Ilievski, Universality Classes of Spin Transport in One-Dimensional Isotropic Magnets: The Onset of Logarithmic Anomalies, Phys. Rev. Lett. **124**, 210605 (2020).

[52] J. S. Ferreira and M. Filippone, Ballistic-to-diffusive transition in spin chains with broken integrability, arXiv:2006.13891.

[53] V. Gorini, A. Kossakowski, and E. C. G. Sudarshan, Completely positive dynamical semigroups of N-level systems, J. Math. Phys. (N.Y.) **17**, 821 (1976).

[54] G. Lindblad, On the generators of quantum dynamical semigroups, Commun. Math. Phys. **48**, 119 (1976).

[55] See Supplemental Material at http://link.aps.org/supplemental/10.1103/PhysRevLett.125.180605 for numerical details, additional data, among other on the single impurity case.

[56] M. Žnidarič, Nonequilibirum steady-state Kubo formula: Equality of transport coefficients, Phys. Rev. B **99**, 035143 (2019).

[57] U. Schollwöck, The density-matrix renormalization group in the age of matrix product states, Ann. Phys. (N.Y.) **326**, 96 (2011).

[58] M. Žnidarič, A. Scardicchio, and V. K. Varma, Diffusive and Subdiffusive Spin Transport in the Ergodic Phase of a Many-Body Localizable System, Phys. Rev. Lett. **117**, 040601 (2016).

[59] M. Horvat and M. Žnidarič, Transport in a disordered tight-binding chain with dephasing, Eur. Phys. J. B **86**, 67 (2013).

[60] A. Metavitsiadis, X. Zotos, O. S. Barišić, and P. Prelovšek, Thermal transport in a spin-1/2 Heisenberg chain coupled

to a magnetic or nonmagnetic impurity, Phys. Rev. B **81**, 205101 (2010).

[61] E. Ilievski, J. De Nardis, M. Medenjak, and T. Prosen, Super-Diffusion in One-Dimensional Quantum Lattice Models, Phys. Rev. Lett. **121**, 230602 (2018).

[62] J. De Nardis, S. Gopalakrishnan, E. Ilievski, and R. Vasseur, Superdiffusion from Emergent Classical Solitons in Quantum Spin Chains, Phys. Rev. Lett. **125**, 070601 (2020).

[63] Ž. Krajnik and T. Prosen, Physics in integrable rotationally symmetric dynamics on discrete spacetime lattice, J. Stat. Phys. **179**, 110 (2020).

[64] V. K. Varma and M. Žnidarič, Diffusive transport in a quasiperiodic Fibonacci chain: Absence of many-body localization at weak interactions, Phys. Rev. B **100**, 085105 (2019).